J|A|C|S
COMMUNICATIONS

Published on Web 01/01/2008

Direct Observation of the Preference of Hole Transfer over Electron Transfer for Radical Ion Pair Recombination in Donor−Bridge−Acceptor Molecules

Zachary E. X. Dance, Michael J. Ahrens, Amy M. Vega, Annie Butler Ricks, David W. McCamant, Mark A. Ratner,* and Michael R. Wasielewski*

Department of Chemistry, Argonne-Northwestern Solar Energy Research (ANSER) Center, and International Institute for Nanotechnology, Northwestern University, Evanston, Illinois 60208-3113

Received September 24, 2007; E-mail: m-wasielewski@northwestern.edu

Understanding how the electronic structures of electron donor−bridge−acceptor (D−B−A) molecules influence the lifetimes of radical ion pairs (RPs) photogenerated within them ($D^{+\bullet}-B-A^{-\bullet}$) is critical to developing molecular systems for solar energy conversion. A general question that often arises is whether the HOMOs or LUMOs of D, B, and A within $D^{+\bullet}-B-A^{-\bullet}$ are primarily involved in charge recombination. If this information is available, molecular structures with properly adjusted energy levels and electronic couplings between states involving these orbitals can be designed to significantly slow energy-wasting charge recombination rates. We recently reported that both photoinduced charge separation and RP recombination for D−B−A molecules in which the acceptor is initially photoexcited, and wherein the bridge molecules are either oligo-*p*-phenylenes (Ph_n) or oligofluorenes, most likely involve charge transfer via the HOMOs of D, B, and A (i.e., hole transfer).[1,2] However, to our knowledge, there is no direct evidence from any D−B−A system that hole transfer is the dominant mechanism of charge recombination. We have developed a new series of D−B−A molecules, which uses a photogenerated charge transfer (CT) state as a high-potential photoreductant to rapidly and nearly quantitatively transfer an electron across an oligo-*p*-phenylene bridge to produce a long-lived RP. Time-resolved EPR (TREPR) spectroscopy shows directly that charge recombination of the RP initially produces a spin-polarized triplet state that can *only* be produced by hole transfer involving the HOMOs of D, B, and A within the D−B−A system.

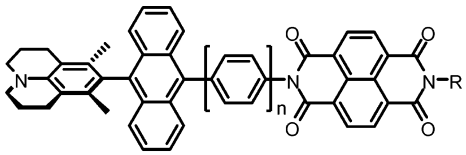

DMJ An Ph NI

1 - 4 (n = 1-4, respectively)

1-3: R = n-C_8H_{17} ; **4**: R = 2,5-di-t-butylphenyl

The D−B−A system consists of a 3,5-dimethyl-4-(9-anthracenyl)julolidine (DMJ-An) electron donor linked to a naphthalene-1,8:4,5-bis(dicarboximide) (NI) acceptor via a series of Ph_n oligomers, where $n = 1-4$, to give DMJ-An-Ph_n-NI, **1**−**4**. DMJ-An is modeled after well-known 4-(9-anthryl)-*N*,*N*-dimethylaniline (ADMA) derivatives[3] but is tailored to produce a high-energy CT excited state that can serve as a good reductant by minimizing molecular motions in the excited state. The nitrogen lone pair in julolidine is conformationally restricted to be parallel to its benzene ring π system, resulting in an electron donor with a reversible oxidation potential of 0.63 V vs SCE, while the methyl groups at the 3 and 5 positions of julolidine strongly constrain its π system to ~90° relative to that of the anthracene. The syntheses of DMJ-An and **1**−**4** are detailed in the Supporting Information.

The lowest excited singlet CT state energy of DMJ-An in toluene, obtained by averaging the energies of its CT absorption and emission maxima at 367 and 519 nm, respectively (Figure S1), is 2.89 eV, while the lifetime of this state measured by time-resolved fluorescence spectroscopy[4] is $\tau = 45.2 \pm 0.1$ ns and its emission quantum yield is 0.31. The CT emission spectrum of DMJ-An is strongly solvatochromic, so that a Lippert−Mataga analysis (see Supporting Information and Figure S2) indicates that direct excitation of the CT absorption band of DMJ-An results in nearly quantitative formation of $^1(DMJ^{+\bullet}\text{-}An^{-\bullet})$. Thus, $An^{-\bullet}$ serves as the electron donor to NI in **1**−**4** ($E_{RED}(An) = -1.97$ V[5] and $E_{RED}(NI) = -0.53$ V[6] vs SCE). The radical ion pair distances and their energies are given in Table S1.

The rate constants for charge separation (k_{CS}) and recombination (k_{CR}) in **1**−**4** in toluene were obtained by transient absorption spectroscopy[1] following selective photoexcitation of the CT band in **1**−**4** with 414 nm, 120 fs (k_{CS}) or 7 ns (k_{CR}) laser pulses. The charge separation reactions for **1**−**4**, $DMJ^{+\bullet}\text{-}An^{-\bullet}\text{-}Ph_n\text{-}NI \rightarrow DMJ^{+\bullet}\text{-}An\text{-}Ph_n\text{-}NI^{-\bullet}$, are all rapid and nearly quantitative (Figure 1), as noted by formation of the prominent absorption bands due to $NI^{-\bullet}$ at 480 and 608 nm.[6] Figure 2 shows the transient absorption spectra and kinetics for charge recombination of $DMJ^{+\bullet}\text{-}An\text{-}Ph_3\text{-}NI^{-\bullet}$ within **3** at 293 K on a 2 μs time scale. The transient spectra of **3** are typical of those observed for **1**−**4** and show that $DMJ^{+\bullet}\text{-}An\text{-}Ph_3\text{-}NI^{-\bullet}$, as monitored at the 480 nm $NI^{-\bullet}$ absorption band, decays to a broad longer-lived absorption at 430−580 nm with $\tau_{CR} = 350 \pm 4$ ns. The nature of this long-lived species was determined by TREPR as detailed below.

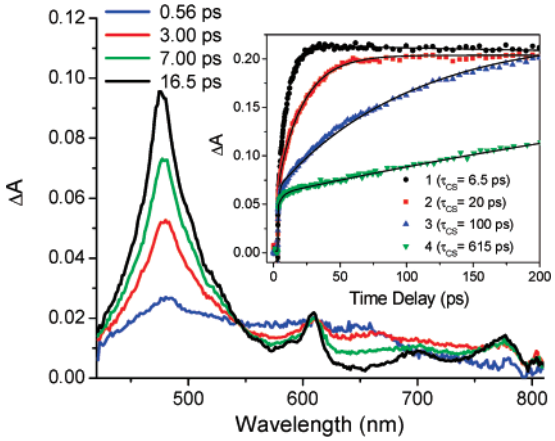

Figure 1. Transient absorption spectra of **1** in toluene at 293 K at the indicated times following a 120 fs, 414 nm laser pulse. Inset: transient absorption kinetics of **1**−**4** in toluene at 293 K at 480 nm following a 120 fs, 414 nm laser pulse. The time constants for the formation of $DMJ^{+\bullet}\text{-}An\text{-}Ph_n\text{-}NI^{-\bullet}$ are given in the inset.

10.1021/ja077386z CCC: $40.75

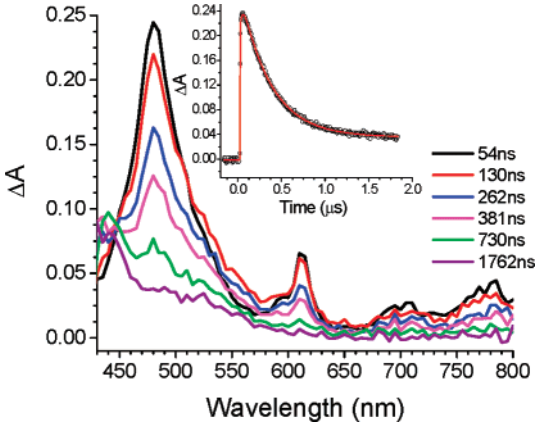

Figure 2. Transient absorption spectra of **3** in toluene at 293 K at the indicated times following a 7 ns, 414 nm laser pulse. Inset: Transient absorption kinetics of **3** in toluene at 480 nm.

Plots of both k_{CS} and k_{CR} versus distance for **1**−**4** at 293 K in toluene (Figure 3) show that these rate constants depend exponentially on distance, which indicates that the superexchange electron-transfer mechanism dominates.[7] The data do not show a switch in mechanism to the charge hopping regime at longer distances as we observed earlier for poly(*p*-phenylene) bridges linking other donors and acceptors.[1,2] For the charge separation reaction, this a consequence of the fact that the energies of the virtual states that place an electron on the bridge (DMJ$^{+\bullet}$-An-Ph$_n^{-\bullet}$-NI) in **1**−**4** (Table S1) are all at least 1 eV higher than that of the initial CT state ^{1}(DMJ$^{+\bullet}$-An$^{-\bullet}$-Ph$_n$-NI). A similar argument holds for charge recombination, where the energies of the virtual states (DMJ-An-Ph$_n^{+\bullet}$-NI$^{-\bullet}$) in **1**−**4** are all at least 0.5 eV higher than those of the fully charge separated state (DMJ$^{+\bullet}$-An-Ph$_n$-NI$^{-\bullet}$).

Following rapid charge separation, the initially formed singlet (S) RP, ^{1}(DMJ$^{+\bullet}$-An-Ph$_n$-NI$^{-\bullet}$), undergoes radical-pair intersystem crossing (RP-ISC)[8,9] induced by electron−nuclear hyperfine coupling within the radicals to produce the triplet RP, ^{3}(DMJ$^{+\bullet}$-An-Ph$_n$-NI$^{-\bullet}$). The TREPR measurements on the RPs were carried out in a 340 mT magnetic field, so that the triplet sublevels of ^{3}(DMJ$^{+\bullet}$-An-Ph$_n$-NI$^{-\bullet}$) undergo Zeeman splitting and are best described by the T_{+1}, T_0, and T_{-1} eigenstates that are quantized along the applied magnetic field.[4,10−12] When RP distances are greater than ∼15 Å, the RP singlet−triplet splitting, *2J* (Figure 4), which depends exponentially on distance, is generally <10 mT, so that the S and

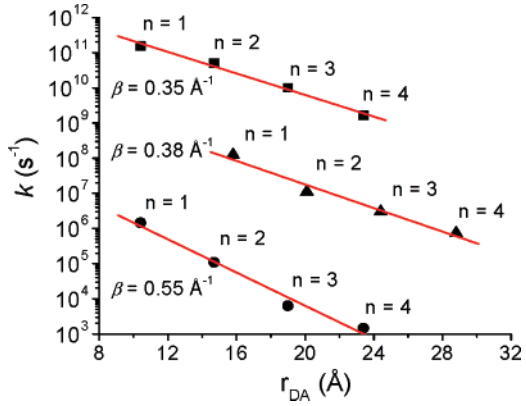

Figure 3. Plots of k_{CS} (■) and k_{CR} (▲) at 293 K and k_{TEnT} (●) at 85 K versus distance, r_{DA}. The red lines are the linear fits to the data. The error bars on the data points are all smaller than the size of the symbols.

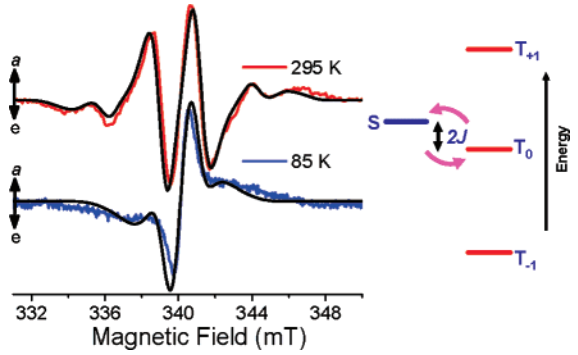

Figure 4. Left: TREPR spectra of **3** in toluene at 300 ns following a 416 nm, 1.5 mJ, 7 ns laser pulse. The black traces are simulations of the data. Right: RP energy levels in the high field limit.

T_0 spin states of the RP are close in energy and mix, while the T_{+1} and T_{-1} states are energetically far removed from the S spin state and do not mix with it.[4,10−12] The two RP states that result from S−T_0 mixing are preferentially populated due to the initial population of S, so that the four EPR transitions that occur between these states and T_{+1} and T_{-1} display a unique spin polarization.[8,9] Thus, the TREPR spectrum consists of two anti-phase doublets, centered at the *g*-factors of the individual radicals that comprise the pair. The splitting in each doublet is determined by *2J* and *D*, the dipolar interaction between the radicals. Resolved hyperfine interactions lead to further splitting of the doublet for each radical. Spin-polarized RP signals were observed by TREPR for **2**−**4** in toluene at both 293 and 85 K, while the RP lifetime for **1** is too short to observe its spectrum by TREPR. For example, the TREPR spectra of **3** (Figure 4) display the overall (*e*,*a*) spin polarization pattern (where *e* = emission, *a* = enhanced absorption; low to high field) diagnostic of a singlet precursor having $2J > 0$.[8,9] Spectral simulations[13] yield $2J = 4.7 \pm 0.3$ mT at 293 K and 1.0 ± 0.2 mT at 85 K with $D \cong 0$.

The subsequent charge recombination process is spin selective; that is, ^{1}(DMJ$^{+\bullet}$-An-Ph$_n$-NI$^{-\bullet}$) recombines to the singlet ground state, while ^{3}(DMJ$^{+\bullet}$-An-Ph$_n$-NI$^{-\bullet}$) recombines to yield the triplet ^{3*}(DMJ-An-Ph$_n$-NI), which acquires the non-Boltzmann spin population of the triplet RP state.[14] The spin polarization of the EPR transitions exhibited by ^{3*}(DMJ-An-Ph$_n$-NI) can be differentiated from those of a triplet state formed by the ordinary spin−orbit intersystem crossing mechanism by the polarization pattern of its six EPR transitions at the canonical (*x*,*y*,*z*) orientations relative to the applied magnetic field. A RP precursor that undergoes the RP-ISC mechanism by S−T_0 mixing followed by charge recombination uniquely yields a (*a*,*e*,*e*,*a*,*a*,*e*) (low field to high field) polarization pattern.[14]

Upon charge recombination, two overlapping broad triplet spectra with widths of ∼150 mT appear in the TREPR spectra of **1**−**4**. Figure 5 shows representative spectra for **3** having the (*a*,*e*,*e*,*a*,*a*,*e*) polarization pattern. The overlapping triplet states have zero field splittings that identify them as ^{3*}An and ^{3*}NI having energies of 1.8[15] and 2.0 eV,[16] respectively. The time-resolved data clearly show that ^{3*}NI is produced *first*, even though both ^{3*}An and ^{3*}NI have lower energies than the RPs (Table S1). These data explicitly show for the first time the *direction* of charge recombination; it occurs by hole transfer via the HOMOs from DMJ$^{+\bullet}$ to NI$^{-\bullet}$ to initially yield ^{3*}NI preferentially rather than occurring by electron transfer via the LUMOs from NI$^{-\bullet}$ to DMJ$^{+\bullet}$ to yield ^{3*}An.

The basis for this preference can be understood by considering the electronic coupling matrix element for the superexchange

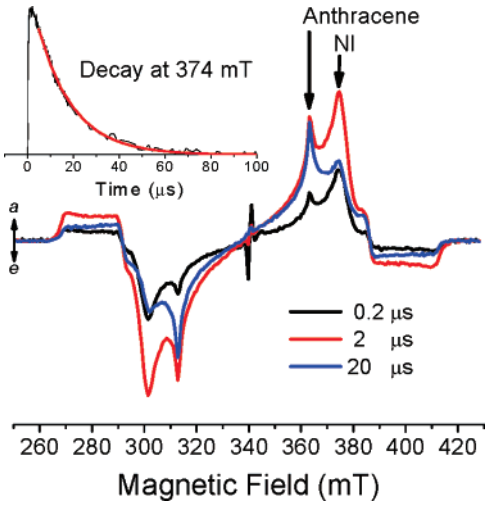

Figure 5. TREPR spectra of **3** in toluene at 85 K at the indicated times following a 416 nm, 7 ns, 1.5 mJ laser pulse. The sharp feature at the center is the radical pair signal, while the broad features are the triplet signals. Inset: kinetics at the indicated magnetic field with the single exponential fit to the data shown in red.

charge-transfer mechanism, V_{DA}, which can be approximated as $V_{DB} \times V_{BA}/\Delta E_{DB}$, where V_{DB} and V_{BA} are the donor−bridge and bridge−acceptor couplings, respectively, and ΔE_{DB} is the donor−bridge energy gap.[7] These parameters are determined primarily by bridge structure and length, conformational rigidity, temperature, and the electronic properties of the redox centers.[1,2,17,18] The energies of all the electronic states with charge formally residing on the bridge in **1**−**4** are high enough that these states remain unpopulated virtual states. However, the values of ΔE_{DB} between $DMJ^{+\bullet}$-An-Ph_n-$NI^{-\bullet}$ and DMJ-An-$Ph_n^{+\bullet}$-$NI^{-\bullet}$ are ∼1.0−1.4 eV smaller than those between $DMJ^{+\bullet}$-An-Ph_n-$NI^{-\bullet}$ and $DMJ^{+\bullet}$-An-$Ph_n^{-\bullet}$-NI (Table S1). As a result, superexchange-mediated hole transfer via the HOMOs is energetically favored over electron transfer via the LUMOs for this D−B−A series.

Following the formation of ^{3*}NI, triplet−triplet energy transfer (TEnT) from ^{3*}NI to ^{3*}An occurs (Figure 5). The TEnT rate constants, k_{TEnT}, were calculated according to the equation, $k_{TEnT} = 1/\tau - 1/\tau_0$, where τ is decay of ^{3*}NI in **2**−**4** and τ_0 is the intrinsic spin relaxation-limited decay time of ^{3*}NI at 85 K (17.1 ± 0.3 μs). TEnT occurs by a Dexter-type mechanism that can be viewed as a pair of simultaneous hole and electron-transfer events involving the HOMOs and LUMOs, respectively, of the D−B−A system. Thus, it is governed by the same parameters used to describe superexchange electron or hole transfer.[19−21] Specifically, k_{TEnT} also displays an exponential distance dependence $k_{TEnT} = k_0 \exp[-\beta(r_{DA} - r_0)]$, where k_0 is the rate constant at van der Waals contact, r_0, r_{DA} is the donor−acceptor center-to-center distance, and β depends on the nature of the bridge and the energy matching between the donor and the bridge.[22,23] Figure 3 shows a plot of ln k_{TEnT} versus r_{DA} for **1**−**4** in which the best fit line through the data points gives $\beta_{TEnT} = 0.55$ Å^{-1}. This value of β_{TEnT} is similar to that obtained from studies of TEnT from $Ru(bpy)_3^{2+}$ to $Os(bpy)_3^{2+}$ through oligo-*p*-phenylenes, where $\beta = 0.50$ Å^{-1}.[24]

Measurements of the β values for hole transfer ($\beta_{HT} = 1.1$ Å^{-1}) and electron transfer ($\beta_{ET} = 1.1$ Å^{-1}) across rigid saturated hydrocarbon spacers have shown that $\beta_{TEnT} \cong \beta_{ET} + \beta_{HT}$ provided that the Franck−Condon-weighted densities of states are similar for these processes.[19−21] The plots of k_{CS} and k_{CR} versus r_{DA} for **1**−**4** in Figure 3 yield $\beta_{CS} = 0.35$ Å^{-1} and $\beta_{CR} = 0.38$ Å^{-1}, respectively. Since the CS and CR reactions within **1**−**4** are ET and HT reactions, respectively, our measured values of β_{CS} and β_{CR} predict that $\beta_{TEnT} = 0.73$ Å^{-1} at 293 K. Interestingly, this value is only modestly larger than $\beta_{TEnT} = 0.55$ Å^{-1} measured at 85 K. The difference between β_{TEnT} obtained from $\beta_{ET} + \beta_{HT}$ and the measured value of β_{TEnT} is not due to the distance dependence of the solvent reorganization energy (λ_S) for CS and CR because λ_S for **1**−**4** in toluene changes by <0.02 eV over the entire range of distances measured (see Supporting Information). However, it may be due to differences in the temperature dependence of β for the charge-transfer reactions relative to that for triplet energy transfer. Previous studies of oligo-*p*-phenylene bridge molecules have shown that β_{TEnT} depends only weakly on temperature,[24] whereas the electronic coupling matrix elements for charge recombination exhibit a stronger temperature dependence.[18] Work is in progress to clarify the detailed temperature dependencies of the charge and energy transfer dynamics of **1**−**4** as well as their analogues having longer and more complex bridge structures.

Acknowledgment. This work was supported by the Chemical Sciences, Geosciences, and Biosciences Division, Office of Basic Energy Sciences, DOE under Grant No. DE-FG02-99ER14999 (M.R.W.), and the NSF Chemistry Division (M.A.R.).

Supporting Information Available: Experimental details including the synthesis and spectra of DMJ-An and **1**−**4**. This material is available free of charge via the Internet at http://pubs.acs.org.

References

(1) Weiss, E. A.; Ahrens, M. J.; Sinks, L. E.; Gusev, A. V.; Ratner, M. A.; Wasielewski, M. R. *J. Am. Chem. Soc.* **2004**, *126*, 5577−5584.
(2) Goldsmith, R. H.; Sinks, L. E.; Kelley, R. F.; Betzen, L. J.; Liu, W. H.; Weiss, E. A.; Ratner, M. A.; Wasielewski, M. R. *Proc. Natl. Acad. Sci. U.S.A.* **2005**, *102*, 3540−3545.
(3) Herbich, J.; Kapturkiewicz, A. *Chem. Phys. Lett.* **1997**, *273*, 9−17.
(4) Dance, Z. E. X.; Mi, Q. X.; McCamant, D. W.; Ahrens, M. J.; Ratner, M. A.; Wasielewski, M. R. *J. Phys. Chem. B* **2006**, *110*, 25163−25173.
(5) Parker, V. D. *J. Am. Chem. Soc.* **1976**, *98*, 98−103.
(6) Gosztola, D.; Niemczyk, M. P.; Svec, W. A.; Lukas, A. S.; Wasielewski, M. R. *J. Phys. Chem. A* **2000**, *104*, 6545−6551.
(7) Jortner, J.; Bixon, M.; Langenbacher, T.; Michel-Beyerle, M. E. *Proc. Natl. Acad. Sci. U.S.A.* **1998**, *95*, 12759−12765.
(8) Closs, G. L.; Forbes, M. D. E.; James, R.; Norris, J. *J. Phys. Chem.* **1987**, *91*, 3592−3599.
(9) Hore, P. J.; Hunter, D. A.; McKie, C. D.; Hoff, A. J. *Chem. Phys. Lett.* **1987**, *137*, 495−500.
(10) Hasharoni, K.; Levanon, H.; Greenfield, S. R.; Gosztola, D. J.; Svec, W. A.; Wasielewski, M. R. *J. Am. Chem. Soc.* **1996**, *118*, 10228−10235.
(11) Carbonera, D.; DiValentin, M.; Corvaja, C.; Agostini, G.; Giacometti, G.; Liddell, P. A.; Kuciauskas, D.; Moore, A. L.; Moore, T. A.; Gust, D. *J. Am. Chem. Soc.* **1998**, *120*, 4398−4405.
(12) Kobori, Y.; Yamauchi, S.; Akiyama, K.; Tero-Kubota, S.; Imahori, H.; Fukuzumi, S.; Norris, J. R., Jr. *Proc. Natl. Acad. Sci. U.S.A.* **2005**, *102*, 10017−10022.
(13) Till, U.; Hore, P. J. *Mol. Phys.* **1997**, *90*, 289−296.
(14) Levanon, H.; Hasharoni, K. *Prog. React. Kinet.* **1995**, *20*, 309−346.
(15) Langelaar, J.; Rettschnick, R. P. H.; Hoijtink, G. J. *J. Chem. Phys.* **1971**, *54*, 1−7.
(16) Wiederrecht, G. P.; Svec, W. A.; Wasielewski, M. R.; Galili, T.; Levanon, H. *J. Am. Chem. Soc.* **2000**, *122*, 9715−9722.
(17) De la Torre, G.; Giacalone, F.; Segura, J. L.; Martin, N.; Guldi, D. M. *Chem.−Eur. J.* **2005**, *11*, 1267−1280.
(18) Weiss, E. A.; Tauber, M. J.; Kelley, R. F.; Ahrens, M. J.; Ratner, M. A.; Wasielewski, M. R. *J. Am. Chem. Soc.* **2005**, *127*, 11842−11850.
(19) Closs, G. L.; Piotrowiak, P.; MacInnis, J. M.; Fleming, G. R. *J. Am. Chem. Soc.* **1988**, *110*, 2652−2653.
(20) Closs, G. L.; Johnson, M. D.; Miller, J. R.; Piotrowiak, P. *J. Am. Chem. Soc.* **1989**, *111*, 3751−3753.
(21) Johnson, M. D.; Miller, J. R.; Green, N. S.; Closs, G. L. *J. Phys. Chem.* **1989**, *93*, 1173−1176.
(22) Andreasson, J.; Kajanus, J.; Mårtensson, J.; Albinsson, B. *J. Am. Chem. Soc.* **2000**, *122*, 9844−9845.
(23) Wiberg, J.; Guo, L.; Pettersson, K.; Nilsson, D.; Ljungdahl, T.; Mårtensson, J.; Albinsson, B. *J. Am. Chem. Soc.* **2007**, *129*, 155−163.
(24) Schlicke, B.; Belser, P.; De Cola, L.; Sabbioni, E.; Balzani, V. *J. Am. Chem. Soc.* **1999**, *121*, 4207−4214.

JA077386Z